

Realistic Counterfactual Explanations for Machine Learning-Controlled Mobile Robots using 2D LiDAR

Sindre Benjamin Remman and Anastasios M. Lekkas

Abstract—This paper presents a novel method for generating realistic counterfactual explanations (CFEs) in machine learning (ML)-based control for mobile robots using 2D LiDAR. ML models, especially artificial neural networks (ANNs), can provide advanced decision-making and control capabilities by learning from data. However, they often function as black boxes, making it challenging to interpret them. This is especially a problem in safety-critical control applications. To generate realistic CFEs, we parameterize the LiDAR space with simple shapes such as circles and rectangles, whose parameters are chosen by a genetic algorithm, and the configurations are transformed into LiDAR data by raycasting. Our model-agnostic approach generates CFEs in the form of synthetic LiDAR data that resembles a base LiDAR state but is modified to produce a pre-defined ML model control output based on a query from the user. We demonstrate our method on a mobile robot, the TurtleBot3, controlled using deep reinforcement learning (DRL) in real-world and simulated scenarios. Our method generates logical and realistic CFEs, which helps to interpret the DRL agent’s decision making. This paper contributes towards advancing explainable AI in mobile robotics, and our method could be a tool for understanding, debugging, and improving ML-based autonomous control.

Index Terms—Deep reinforcement learning, Explainable artificial intelligence, Machine learning, Counterfactual explanations, LiDAR, Mobile Robots

I. INTRODUCTION

With the rapid progress of Machine Learning (ML) applications in robotics [1], it is crucial to ensure that the decision-making by ML models is transparent [2]. In safety-critical control tasks, model interpretability can help us understand and trust the control decisions of robots controlled using neural networks, which often function like black boxes. Counterfactual Explanations (CFEs), also called counterfactuals, produce contrastive explanations by showing how small input changes to an ML model can lead to different outputs. CFEs are a promising way to increase interpretability through “what if” scenarios [3].

CFEs have been used in robotics, for instance, in [4], which uses them to assess robot control robustness. The authors train a generative model to create small and realistic modifications to a base image to produce user-defined effects in an image-based controller, thus producing CFEs. These CFEs are then employed as a measurement of the robustness of the controller, i.e., if the CFEs have to be very different from the base image to produce significantly different effects in the controller, the controller is likely robust. Another application is presented in [5], where real-time CFEs are

generated for robotic systems with multiple continuous outputs. The authors use linear model trees to produce the CFEs and demonstrate that while the method might find infeasible CFEs if the input features are not independent, they can perform feature engineering to ensure the input features are independent. Although not robotics, [6] propose a novel solution for generating CFEs for image-input-based deep reinforcement learning (DRL) agents. They use a saliency map to discover the most important input pixels and use this as input to a generative model that generates realistic CFEs.

While there has been work on CFEs in robotics and DRL, to our knowledge, no existing methods deal with CFEs for high-dimensional LiDAR data. In this paper, we demonstrate how applying Diverse Counterfactual Explanations (DiCE), an existing CFE generation method to LiDAR data can lead to noisy and unrealistic results due to the correlations often present between neighboring readings in LiDAR data. We propose a model-agnostic approach for generating realistic CFEs tailored for mobile robots with 2D LiDAR. Although demonstrated here with an ML-based controller, this method could also be used for traditional control algorithms because of its model-agnostic workings. By parameterizing the LiDAR space with geometric shapes, we ensure the CFEs resemble realistic environments. Our method can, therefore, give a true and intuitive understanding of a model’s decision-making. We test our method on a TurtleBot3 with a DRL policy in both simulated and real-world settings. Our method surpasses existing techniques like DiCE in interpretability and similarity to real data when applied to 2D LiDAR data.

Our contributions include:

- A novel, model-agnostic method for generating spatially realistic CFEs for robots with 2D LiDAR, which applies a genetic algorithm approach inspired by DiCE, with significant modifications to handle the spatial structure of LiDAR data.
- A comparison against DiCE, demonstrating enhanced interpretability and realism for 2D LiDAR data.
- Real-world tests on a TurtleBot3 controlled by DRL, demonstrating the method’s applicability to control tasks and its effectiveness with real-world data.
- An experiment using generated LiDAR-like data to investigate the ML model’s behavior preferences, demonstrating how our methodology can improve understanding of ML models.

II. BACKGROUND AND THEORY

This section introduces CFEs and genetic algorithms, which are important concepts in our approach. CFEs help interpret ML models by showing how small input changes

The authors are with the Department of Engineering Cybernetics, Norwegian University of Science and Technology (NTNU), Trondheim, Norway {sindre.b.remman, anastasios.lekkas}@ntnu.no

affect outcomes based on user queries. Genetic algorithms are the optimization methods that we use to generate our CFEs. We discuss how the methodology uses these concepts in Section III.

A. Counterfactual Explanations

Effective explanations are often *contrastive*, and answer questions like, "Why not this instead?" rather than simply "Why?" [7], [8]. In ML, CFEs are particularly suited for this since they show how changes in input can produce different, user-defined outcomes. For instance, in a model classifying images of cats and dogs, a CFE could explain how an image of a cat would need to change to be labeled as a dog.

In robotics, CFEs can answer questions like "What changes could make the model choose action B over action A ?" The continuous action spaces in robotics make it difficult to find precise numerical outputs, so it is more relevant to ask, "What changes could make the model choose an action within bounds B rather than a specific action A ?"

Inspired by DiCE's approach [9], we define CFEs for continuous outputs as follows: Let $\mathbf{x} \in \mathbb{R}^n$ represent the input space and $f: \mathbb{R}^n \rightarrow \mathbb{R}^m$ be the ML model, mapping inputs to actions $\mathbf{a} = f(\mathbf{x}) \in \mathbb{R}^m$. For a target action bound $\mathbf{B} \subset \mathbb{R}^m$, a CFE \mathbf{x}_{cf} is an adjusted input such that:

$$f(\mathbf{x}_{cf}) \in \mathbf{B} \quad \text{and} \quad \|\mathbf{x} - \mathbf{x}_{cf}\| \leq \epsilon,$$

where $f(\mathbf{x}_{cf})$ is inside the target bounds \mathbf{B} with minimal deviation ϵ from the original input \mathbf{x} .

B. Genetic Algorithms

Genetic algorithms (GAs), introduced by Holland in [10], are optimization methods inspired by natural selection, suited to non-linear, non-convex problems [11]. Our approach uses a GA to optimize candidate solutions, or individuals, for generating realistic LiDAR CFEs. The whole set of candidate solutions is called the population. It consists of individuals structured as chromosomes, composed of genes that encode specific parameters and are evaluated by a fitness function, also called an objective function.

To evolve the population, a GA uses three main operators [11]:

- *Crossover*: Generates offspring by combining genes from two or more parents.
- *Mutation*: Maintains diversity between generations by introducing random changes.
- *Elitism*: Keeps the best solutions between generations to have steady progress.

The GA iterates through several steps: initialization of a random population, evaluation of each individual's fitness, selection for crossover and mutation, and replacement to form the next generation. Elitism ensures that high-quality solutions are preserved and that solutions are steadily progressing. This process continues until a stopping criterion is met, such as reaching a maximum number of generations or achieving a certain fitness score.

III. METHODOLOGY

A. Generating Realistic LiDAR Counterfactuals

In our algorithm, detailed below, we use *real* and *virtual* LiDAR data. Real LiDAR data consists of sensor readings, the distances from the LiDAR to the closest objects at certain angle intervals 360 degrees around the sensor, collected directly from the environment. On the other hand, virtual LiDAR data is artificially generated to simulate hypothetical obstacles and configurations. This virtual data forms the basis of our CFEs, showing how modified sensor inputs could affect the model's decisions.

Generating realistic CFEs from LiDAR data is challenging due to spatial correlations. For instance, consecutive LiDAR readings may reflect the same object. CFEs generated without considering these correlations tend to resemble noise, as we demonstrate with the DiCE method in Section IV-A.

Our methodology generates LiDAR CFEs by modifying sensor readings to illustrate how small and realistic changes can lead to different model outputs. In our case study, shown in Section III-B, the ML model, f , selects linear and angular velocities directly from LiDAR data. To generate realistic CFEs, we parameterize the LiDAR space with basic shapes (e.g., circles, squares) and transform these into virtual LiDAR data by raycasting to the shapes' boundaries, using the Shapely package [12]. Once generated, these virtual LiDAR points are combined with the original LiDAR state using two combination methods, illustrated in Figure 1 and explained below.

Let \mathbf{b} and \mathbf{c} represent vectors of LiDAR readings in meters, where:

- $\mathbf{b} = [b_1, b_2, \dots, b_n]$ denotes the baseline LiDAR readings, and
- $\mathbf{c} = [c_1, c_2, \dots, c_n]$ denotes the generated LiDAR readings corresponding to the obstacles.

The first combination method, which we call *min_distance*, computes a new vector \mathbf{d} by taking the minimum value for each entry in \mathbf{b} and \mathbf{c} , which element-wise is:

$$d_i = \min(b_i, c_i) \quad \text{for } i = 1, 2, \dots, n. \quad (1)$$

The second combination method, called *gen_priority*, prioritizes the generated readings, \mathbf{c} , whenever they fall within a specified threshold distance, D_{\max} , which represents the maximum LiDAR range. This approach results in combined LiDAR readings that match the generated readings when a LiDAR ray would encounter a generated obstacle and defaults to baseline readings otherwise. This is defined element-wise as:

$$d_i = \begin{cases} c_i & \text{if } c_i < D_{\max}, \\ b_i & \text{otherwise.} \end{cases} \quad \text{for } i = 1, 2, \dots, n. \quad (2)$$

Each of the two combination methods provides a different approach to combining baseline and generated LiDAR data to generate a LiDAR state that serves as the CFE instance. The *min_distance* combination method represents what would happen if we placed the generated obstacles in the environment without changing anything else, which can make the CFEs more actionable. On the other hand,

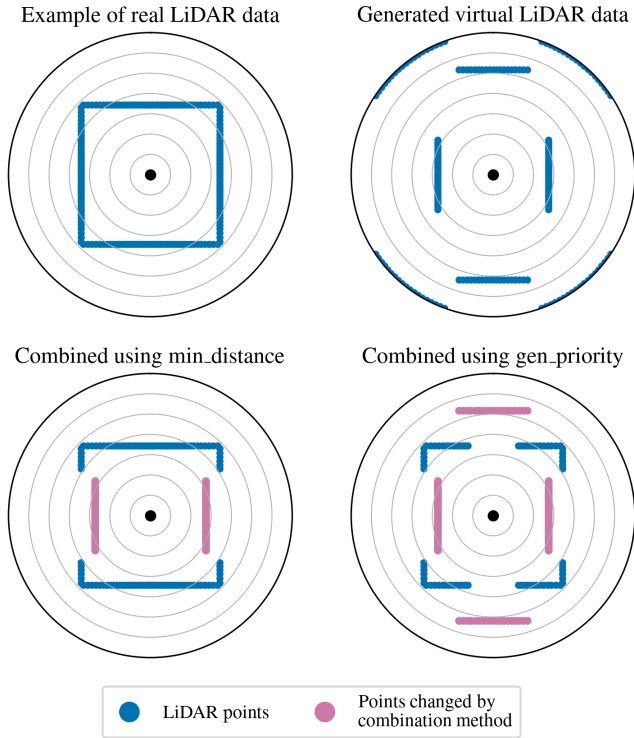


Fig. 1: Example illustrating the two combination methods. The top left shows the base LiDAR state with four walls around the sensor, while the top right shows the generated virtual obstacles. The lower left shows the result of combining these data with *min_distance*, which keeps the nearest obstacles at each reading, and the lower right shows *gen_priority*, which prioritizes the virtual obstacles. The dot at the center marks the origin of the LiDAR sensor.

TABLE I: Genetic Algorithm Parameters for PyGAD

| Parameter | Value/Description |
|--------------------------|----------------------------|
| Number of Generations | 100 |
| Number of Parents Mating | 10 |
| Solutions per Population | 100 |
| Parent Selection Type | Tournament |
| Keep Parents | 10 |
| Crossover Type | Single-point |
| Mutation Type | Random |
| Mutation Percent Genes | 20% |
| Stop Criteria | {"saturate_10", "reach_0"} |

gen_priority gives the algorithm more freedom by letting it make larger changes from the base state.

The methodology's main challenge is placing the virtual obstacles so that a specific change in the ML model's output is achieved. Since raycasting and ML models, such as neural networks, are generally non-linear and non-convex, we use a GA rather than gradient-based optimization. To implement the GA, we use the PyGAD Python package [13] with parameters shown in Table I, where we use a mutation rate of 20% to increase the chance of discovering diverse solutions. Our full implementation is available in [14].

We define the gene space for the GA to encode each virtual obstacle using six genes, representing obstacle type, circle or rectangle here (one gene), position and orientation

(three genes), and size (two genes). For circles, we ignore the orientation gene and one of the size genes. Each gene value is normalized between 0 and 1. If we have o_n obstacles to generate, the gene space is then of size $o_n \times 6$.

Each chromosome, representing a specific configuration of obstacles, is evaluated by the fitness function shown in Algorithm 1 to calculate how well each candidate fulfills the requirements. This fitness function uses two loss functions, inspired by DiCE's approach: hinge loss, y_{loss} , and proximity loss, p_{loss} :

$$y_{\text{loss}} = \begin{cases} 0, & \text{if } B_0 \leq \hat{y} \leq B_1, \\ \min(|\hat{y} - B_0|, |\hat{y} - B_1|), & \text{otherwise.} \end{cases} \quad (3)$$

- y_{loss} : Hinge loss
- \hat{y} : Output of the ML model
- B_0 and B_1 : Lower and upper bounds of the desired range for \hat{y} .

$$p_{\text{loss}} = - \sum_{i=1}^n |d_i - b_i| \quad (4)$$

- d_i represents each element in the model input (i.e., the generated LiDAR data),
- b_i is the corresponding element in the baseline state,
- n is the dimension of the state.

The hinge loss encourages the output of the ML model to be within the user-defined bounds, and the proximity loss encourages the generated solution's LiDAR representation to be close to the base state.

After running the GA and receiving the solutions, we only need to decode and combine the solutions with the base LiDAR state using the selected combination function to receive our CFEs.

Algorithm 1 Realistic LiDAR CFE Fitness Function

Require: Solution s , Baseline data \mathbf{b} , Output bounds B , Combination function F , ML model P , y_{loss} weight λ_y , p_{loss} weight λ_p , Min distance from LiDAR d_{\min}

Ensure: Fitness score $f(s)$

- 1: Decode solution s into spatial parameters for each obstacles, including type, size, position, and orientation.
- 2: **If** any obstacle overlap a circle with radius d_{\min} centered at the LiDAR origin, **then return** $f(s) \leftarrow -\infty$
- 3: Generate LiDAR data \mathbf{c} from the generated obstacles using raycasting.
- 4: Combine baseline \mathbf{b} and generated \mathbf{c} to obtain combined LiDAR state \mathbf{d} using F .
- 5: **Initialize** $f(s) \leftarrow 0$ ▷ Initialize fitness score to zero
- 6: Input combined state \mathbf{d} to model P to obtain output \mathbf{y} .
- 7: Calculate $y_{i,\text{loss}}$ for each y_i in \mathbf{y} using Equation (3).
- 8: $f(s) \leftarrow f(s) - \sum_i \lambda_y \cdot y_{i,\text{loss}}$.
- 9: Calculate p_{loss} between \mathbf{d} and \mathbf{b} using Equation (4).
- 10: Normalize p_{loss} over the LiDAR dimension.
- 11: $f(s) \leftarrow f(s) - \lambda_p \cdot p_{\text{loss}}$.
- 12: **return** $f(s)$

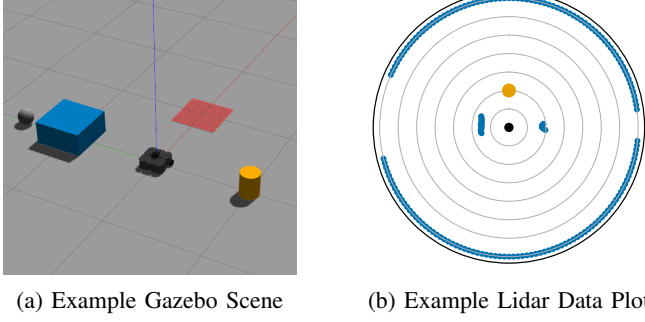


Fig. 2: Example of a Gazebo scene and the corresponding LiDAR plot. The goal in front of the TurtleBot3 is shown as a red square in Gazebo and an orange circle in the LiDAR plot. The TurtleBot3 is represented by the black dot in the middle of the plot, the blue square to the left of the TurtleBot3 is shown to the left of the TurtleBot3 in the plot, and vice versa with the orange cylinder to the right. The grey sphere is not visible in Figure 2b since it is behind the blue cube and not visible from the TurtleBot3's point of view.

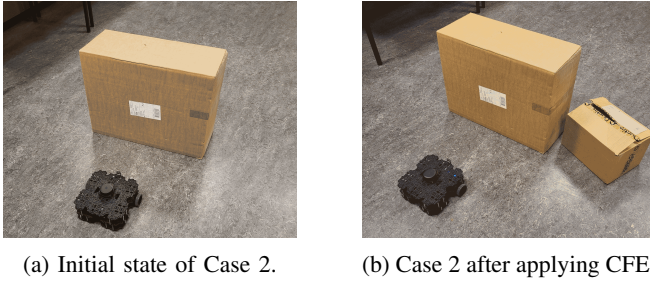


Fig. 3: Photos of the real-world setup for Case 2, before and after actualizing the CFE, discussed in Section IV-B.2.

B. TurtleBot3 case study

To evaluate our algorithm, we use the TurtleBot3¹, a low-cost, versatile mobile robot platform widely used in research and education. It has a 360-degree 2D LiDAR and is also integrated with Robot Operating System (ROS), which streamlines the controlling of the mobile robot. Figure 2 shows the TurtleBot3 in a Gazebo scene and the corresponding LiDAR plot. We use these types of plots throughout this paper. We conduct experiments in a large room to test our algorithm on real-world data, and we place cardboard boxes to recreate the CFEs generated by our method. An example of this real-world environment can be seen in Figure 3.

The ML model controlling the TurtleBot3 is a DRL model, trained using the Stable-Baselines3 implementation of the Soft Actor-Critic (SAC) algorithm [15], [16]. To help the agent adapt to new environments, we train the model using domain randomization [17] to generate random environments in the Gazebo simulator [18]. Our ROS package for generating these environments is available at [19].

We formulate this as a reinforcement learning (RL) problem, extending our previous work in [20], where the goal is to navigate the TurtleBot3 to a specific location. We define the state space \mathbf{s} as:

- $\mathbf{s}_{\text{LiDAR}} = [s_1, s_2, \dots, s_{180}]$: A vector of 180 LiDAR distance readings collected at 2-degree intervals 360 degrees around the TurtleBot3,
- $\cos(\theta_g)$: The cosine of the angle to the goal,
- $\sin(\theta_g)$: The sine of the angle to the goal,
- d_g : The distance to the goal from the TurtleBot3.

All elements of \mathbf{s} are normalized to lie within the range $[0, 1]$.

The action space $\mathbf{a} = [a_{\text{linear}}, a_{\text{angular}}]$ is defined as:

- a_{linear} : The applied linear velocity of the TurtleBot3,
- a_{angular} : The applied angular velocity.

Both actions are scaled between $[-1, 1]$ using a hyperbolic tangent (tanh) activation function in the output layer, and multiplied by their respective maximum values for the TurtleBot3. These scaled commands are sent to the robot using messages to the `vel_cmd` ROS topic.

The reward function we used, which we found using trial and error, is

$$R = (-d_{\text{current}}) + \lambda_{\text{obstacle}} \cdot e^{-k \cdot \min(\mathbf{s}_{\text{LiDAR}})} + \lambda_{\text{backwards}} \cdot a_{\text{linear}}, \quad (5)$$

where:

- d_{current} is the current distance to the goal,
- $\lambda_{\text{obstacle}} = -2.0$: Penalizes proximity to obstacles.
- $k = 50.0$: Controls the steepness of the exponential obstacle penalty.
- $\lambda_{\text{backwards}} = 0.01$: Penalizes backward movement.
- $\mathbf{s}_{\text{LiDAR}}$ represents the vector of LiDAR readings, with $\min(\mathbf{s}_{\text{LiDAR}})$ as the distance to the closest obstacle,
- a_{linear} is the linear component of the action, with a penalty applied if moving *backward*.

In addition, when the agent crashes or reaches the goal, it gets an additional reward of -100 or +100.

While traditional control methods could solve this navigation task, by using DRL, we create a good test case study for our CFE generation algorithm. In addition, this task is a Partially Observable Markov Decision Process (POMDP), where solutions typically benefit from a memory of past states. However, for this case study, we simplify using only convolutional and feedforward layers, without recurrent elements, to simplify training and implementation and focus on testing the CFE generation method.

To find optimal hyperparameters for training, we use Optuna [21] for hyperparameter tuning. The search space for SAC and the final values are shown in Table II and Table III, respectively.

Our neural network first processes the 180 LiDAR readings through two 1D convolutional layers using **circular padding**. The first layer has **4 output channels**, a **kernel size of 5**, **stride of 1**, and **padding of 2**. The second layer has **8 output channels**, a **kernel size of 5**, **stride of 2**, and **padding of 2**. The output is then combined with non-LiDAR inputs and passed through two fully connected layers with **128 units** each. We use ReLU activation functions, except for the tanh output layer.

¹<https://emanual.robotis.com/docs/en/platform/turtlebot3/overview/>

TABLE II: Hyperparameter search space for tuning the Stable-Baselines3 implementation of SAC using Optuna

| Hyperparameter | Range/Values |
|---------------------|---------------------------------------|
| γ | [0.9, 0.9999] (log) |
| Learning Rate | [1e-4, 1e-2] (log) |
| Buffer Size | [600,000, 1,000,000] |
| Batch Size | [16, 400] |
| τ | [1e-3, 1] (log) |
| Entropy Coefficient | {auto, 0.1, 0.01, 0.001, 0.05, 0.005} |
| Target Entropy | {auto, -1, -2, -5, -10} |
| Use SDE | {False, True} |
| Log Std Init | [-3, -0.5] |

TABLE III: Optimized Hyperparameter Values

| Hyperparameter | Final Value |
|---------------------|-------------|
| γ | 0.9856 |
| Learning Rate | 0.0009998 |
| Buffer Size | 747,034 |
| Batch Size | 220 |
| τ | 0.1568 |
| Entropy Coefficient | 0.01 |
| Target Entropy | -2 |
| Use SDE | True |
| Log Std Init | -3.18 |

IV. RESULTS AND DISCUSSION

A. Comparison with DiCE

We compare our LiDAR CFE generation methodology with the DiCE method by Mothilal et al. [22], using the Interpretml implementation [9]. The version of DiCE we use also uses a genetic algorithm for cost function optimization. We had to make alterations in the code to support multi-output regression models. For instance, we adapted the hinge loss described in Equation (3) by summing the hinge losses across output nodes.

We tested both methods in a scenario using generated LiDAR data where walls are positioned to the left and right of the TurtleBot3, with the goal ahead. The base state's LiDAR readings are shown in Figure 4a. In this state, the policy applies the action²

$$\mathbf{a} = [a_{\text{linear}}, a_{\text{angular}}] = [0.9640, 0.4211].$$

To investigate what environmental changes would cause the agent to reverse, we ran both DiCE and our algorithm with desired action bounds of $a_{\text{linear}} \in [-1.0, 0.0]$ and $a_{\text{angular}} \in [-0.1, 0.1]$. In this case, a rational CFE could explain that a large obstacle between the agent and the goal would cause the agent to reverse. Figure 4b shows a CFE generated by DiCE, and Figure 4c presents one generated by our method. The DiCE CFE appears noisy, but our method produces a realistic environment. Adjusting proximity and sparsity weights in DiCE to, in theory, increase the similarity to the base state still resulted in noisy CFEs. Some possible reasons for DiCE's poorer performance include the high dimensionality of the LiDAR data (180 features), which our method works its way around by parameterizing the LiDAR space with the generated obstacles and exploiting spatial correlations between readings through the geometric objects.

²This action also causes a small left turn because the policy prefers to approach the goal from the left in this case.

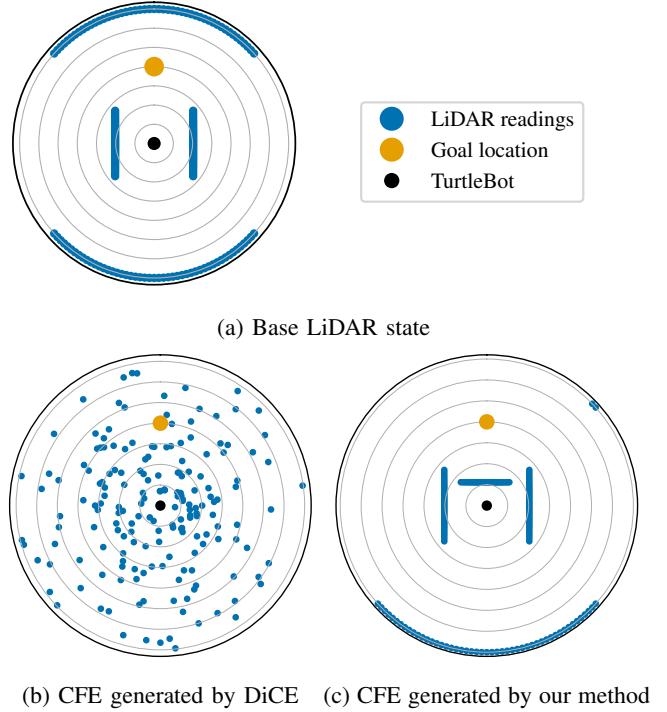


Fig. 4: Comparison between DiCE and our algorithm on a simple case where the goal is right in front, with walls on either side.

Although this comparison may arguably be biased towards our method, it highlights the value of domain knowledge in designing CFE algorithms for specific data types. It could be interesting to try other optimization options within the DiCE package to see if they produce more realistic CFEs, but this is outside the scope of this paper and would require further adaptations for multi-output regression.

B. Real-world experiments

1) *Case 1: No Obstacles*: In this first test using real-world LiDAR data, we generate CFEs for a scenario with no obstacles, and the goal is straight ahead. We define the counterfactual action as moving backward and run our algorithm with the parameters in Table IV. Since similarity to the base state is not important here, we set p_{loss} weight $\lambda_p = 0.0$ and use the *min_distance* combination function, which simplifies obstacle placement.

We generate ten CFEs and display four in Figure 5. Each shows that placing an obstacle directly in front of the TurtleBot3 leads the agent to choose to reverse, as expected. If obstacles only placed behind the agent could lead it to choose a reverse action, this could indicate irrational behavior and suggest a lack of model reliability.

To validate the generated CFEs in Figure 5, we placed a cardboard box similar to the obstacle in Counterfactual 3. We then let the agent navigate to the goal and plot its path in Figure 6 and chosen actions in Figure 7. The TurtleBot3 begins by reversing, as the generated CFE said. The angular velocity action seems noisy, likely due to differences between the simulation the agent was trained in and the real-world environment.

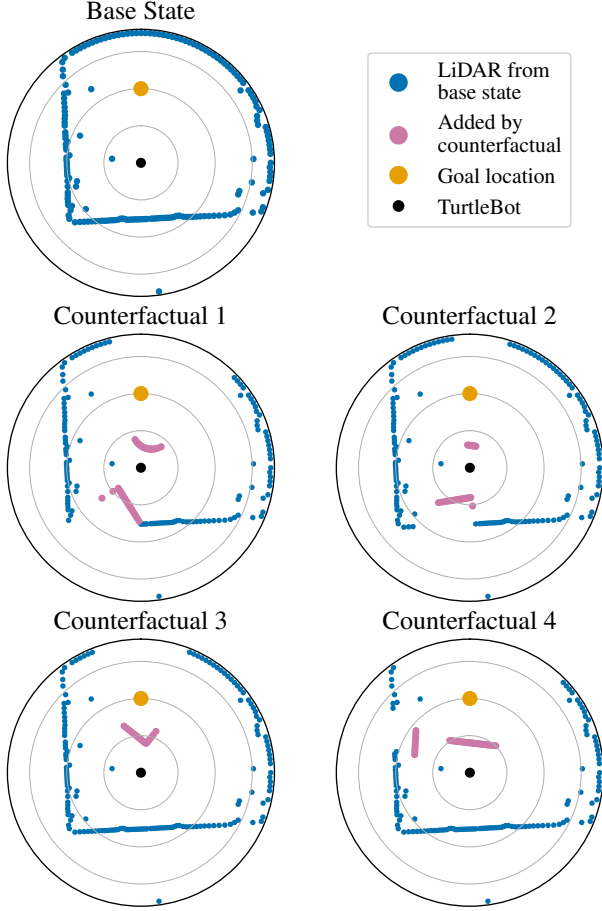


Fig. 5: Four CFEs generated by the algorithm from the base state in Case 1, with the desired action being to move backwards, and not turn much, which we define by $[a_{\text{linear}} \in [-1.0, 0.0]]$ and $a_{\text{angular}} \in [-0.2, 0.2]$.

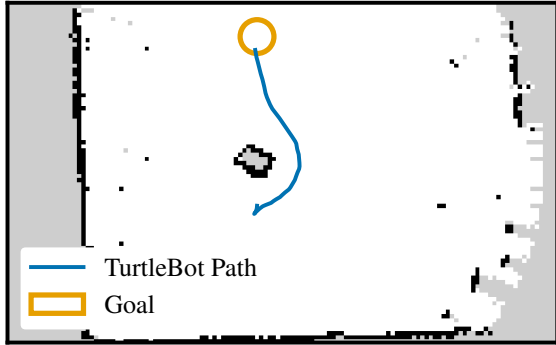


Fig. 6: TurtleBot3 path on a map after adding an obstacle inspired by Counterfactual 3 in Figure 5.

TABLE IV: Case 1, Algorithm Parameters and Results

| Parameter | Value |
|---------------------------------------|---------------|
| Time to Calculate | 205.51 s |
| Combination method | min_distance |
| a_{linear} desired bounds | $[-1.0, 0.0]$ |
| a_{angular} desired bounds | $[-0.2, 0.2]$ |
| y_{loss} weight, λ_y | 1.0 |
| p_{loss} weight, λ_p | 0.0 |
| Number of obstacles generated | 5 |

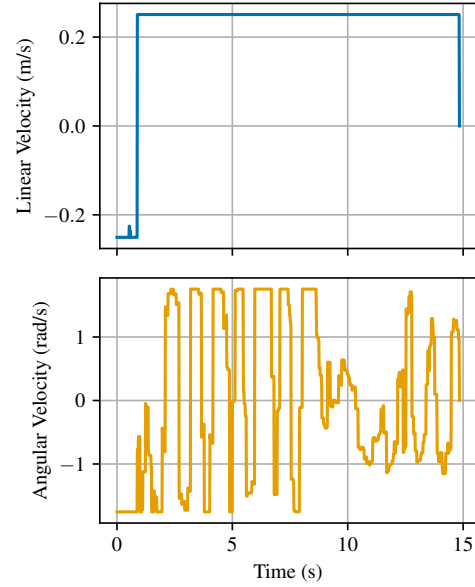


Fig. 7: Actions chosen when we actualize counterfactual 3 in Figure 5.

2) *Case 2: Adding Obstacles to Trick the Agent into Crashing:* In the second case, we attempt to exploit the CFEs to create a scenario where the policy crashes the TurtleBot3. We place a large cardboard box directly in front of the TurtleBot3 and use this as the base state. In this base state, the policy chooses to reverse to the left. To encourage the TurtleBot3 to move forward and potentially crash, we generate CFEs for what it would take to make the agent drive forward instead. To generate the CFEs, we use the parameters in Table V. The base state and generated CFEs are shown in Figure 8, and we select Counterfactual 2 for testing. Figure 3 shows pictures of how the base state and Counterfactual 2 looks in the real world.

Counterfactual 2 suggests adding more obstacles in front of the TurtleBot3, which seems not to be logical for causing the agent to drive forward. We place an additional small box slightly to the right of the larger box and observe the resulting path in Figure 9. Although the TurtleBot3 initially moves forward, it avoids the obstacles, making slight maneuvers around them. This illustrates a limitation of our method and CFEs in general for explaining sequential decision processes: an agent's action in one step may not predict its subsequent behavior.

TABLE V: Case 2, Algorithm Parameters and Results

| Parameter | Value |
|---------------------------------------|--------------|
| Time to Calculate | 39.84 s |
| Combination method | min_distance |
| a_{linear} desired bounds | [0.6, 1.0] |
| a_{angular} desired bounds | [-1.0, 1.0] |
| y_{loss} weight, λ_y | 1.0 |
| p_{loss} weight, λ_p | 0.0 |
| Number of obstacles generated | 5 |

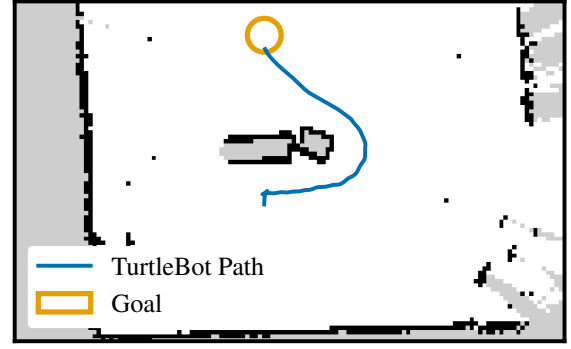


Fig. 9: TurtleBot3 path on a map after adding an obstacle inspired by Counterfactual 2 in Figure 5. Notice the two obstacles in the middle of the map, which are the two cardboard boxes added.

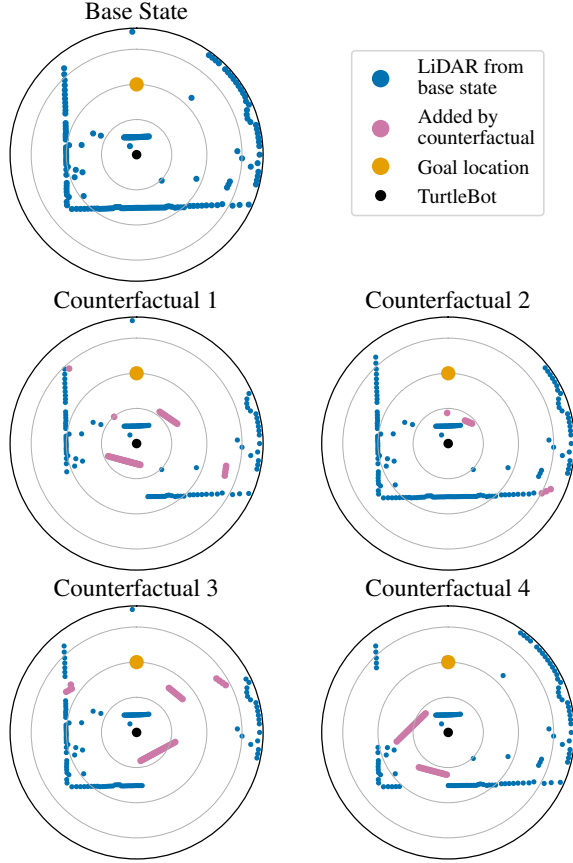
Fig. 8: Four CFEs generated by the algorithm from the base state in Case 2. We aim to make the policy drive the TurtleBot3 forward, which we define by $[a_{\text{linear}} \in [0.6, 1.0]]$ and $a_{\text{angular}} \in [-1.0, 1.0]$.

TABLE VI: Case 3, Algorithm Parameters

| Parameter | Value |
|---------------------------------------|--------------|
| Combination method | min_distance |
| a_{linear} desired bounds | [0.9, 1.0] |
| a_{angular} desired bounds | [-1.0, -0.5] |
| y_{loss} weight, λ_y | 1.0 |
| p_{loss} weight, λ_p | 0.1 |
| Number of obstacles generated | 1 |

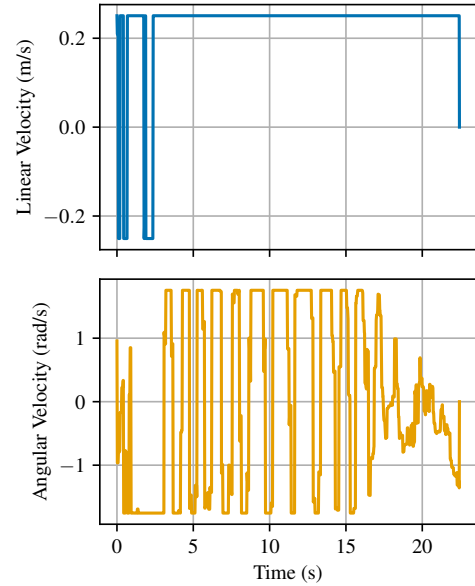


Fig. 10: Actions chosen when we actualize counterfactual 2 in Figure 5.

C. Case 3: Explaining the Policy's Left-Turn Preference

After observing that our DRL policy often prefers to turn to the left, we try to gain an understanding of this by generating CFEs. Using virtual data, we simulate a base LiDAR state with a box obstacle 2.5 meters in front of the LiDAR origin (shown in the top left of Figure 11), where the policy selects the action

$$\mathbf{a} = [a_{\text{linear}}, a_{\text{angular}}] = [0.9640, 0.9640].$$

We run our algorithm with the parameters in Table VI and generate 100 CFEs, selecting $\lambda_p = 0.1$, to ensure more similarity to the base state. Four of the generated CFEs are shown in Figure 11. In all 100 generated CFEs, there were only obstacles on the left, even when we set $\lambda_p = 0$ as in the other cases. This result shows that the "base decision" for the agent in this case is to turn to the left and would only not do so if there was an obstacle in the way. Even though these explanations might seem obvious, obvious

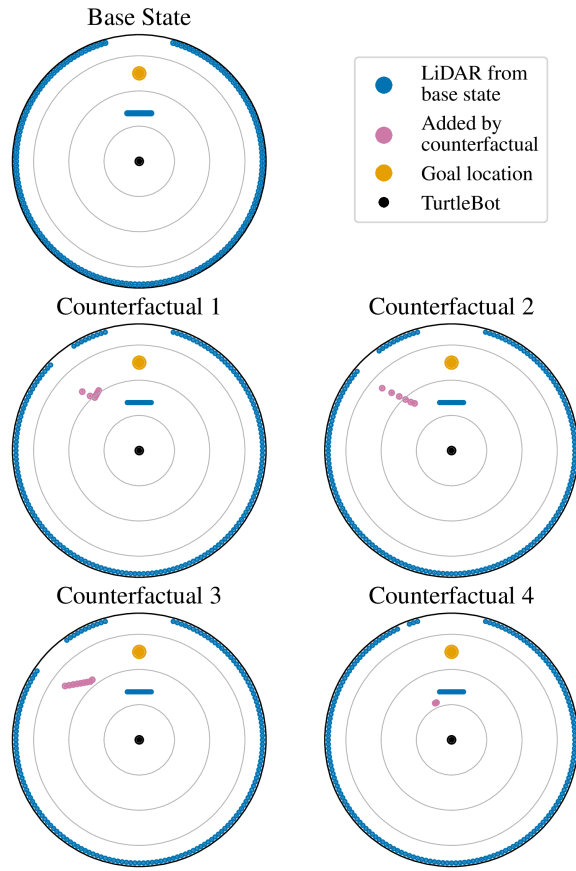


Fig. 11: Base state and CFEs for Case 3

explanations demonstrate our methodology’s strengths and that the agent behaves, at least to some extent, according to human intuition. In this case, we could interpret the user’s question and method’s explanation in natural language as:

User: “Why don’t you turn to the *right* here?”

Agent: “I would turn to the *right* instead of to the *left* if there was an obstacle on the *left*.”

V. CONCLUSION

In this paper, we introduced a method for generating realistic CFEs for ML-controlled mobile robots using 2D LiDAR data to make them more interpretable. Our approach uses genetic algorithms and domain-specific insights to produce realistically structured LiDAR CFEs that are intuitive and give us a good understanding of the ML model’s control decisions.

We perform experiments with a TurtleBot3 controlled using DRL in both simulated and real-world environments to demonstrate how the method can generate realistic CFEs that improve understanding of autonomous control behavior. This work contributes to advancing explainable AI in mobile robotics, and our method can serve as a tool for enhancing transparency and reliability in both ML-based and traditional control systems. Future work could extend this approach to 3D LiDAR, other controllers, and other robotic applications.

ACKNOWLEDGMENT

The Research Council of Norway supported this work through the EXAIGON project, project number 304843.

REFERENCES

- [1] M. Soori, B. Arezoo, and R. Dastres, “Artificial intelligence, machine learning and deep learning in advanced robotics, a review,” *Cognitive Robotics*, vol. 3, pp. 54–70, 2023.
- [2] S. Wachter, B. Mittelstadt, and L. Floridi, “Transparent, explainable, and accountable AI for robotics,” *Science Robotics*, vol. 2, no. 6, 2017, ean6080.
- [3] S. Wachter, B. Mittelstadt, and C. Russell, “Counterfactual explanations without opening the black box: Automated decisions and the GDPR,” *Harvard Journal of Law & Technology*, vol. 31, p. 841, 2017.
- [4] S. C. Smith and S. Ramamoorthy, “Counterfactual explanation and causal inference in service of robustness in robot control,” in *2020 Joint IEEE 10th International Conference on Development and Learning and Epigenetic Robotics (ICDL-EpiRob)*. IEEE, 2020, pp. 1–8.
- [5] V. B. Gjørsum, I. Strümke, A. M. Lekkas, and T. Miller, “Real-time counterfactual explanations for robotic systems with multiple continuous outputs,” *IFAC-PapersOnLine*, vol. 56, no. 2, pp. 7–12, 2023.
- [6] A. Samadi, K. Koufos, K. Debattista, and M. Dianati, “SAFE-RL: Saliency-aware counterfactual explainer for deep reinforcement learning policies,” *IEEE Robotics and Automation Letters*, vol. 56, pp. 9994–10 001, 2024.
- [7] T. Miller, “Explanation in artificial intelligence: Insights from the social sciences,” *Artificial Intelligence*, vol. 267, pp. 1–38, 2019.
- [8] C. Molnar, *Interpretable Machine Learning*, 2nd ed., 2022. [Online]. Available: <https://christophm.github.io/interpretable-ml-book>
- [9] R. Mothilal, A. Sharma, and C. Tan, “DiCE: Diverse Counterfactual Explanations,” 2020. [Online]. Available: <https://github.com/interpretml/DiCE>
- [10] J. H. Holland, *Adaptation in Natural and Artificial Systems*. University of Michigan Press, 1975.
- [11] S. Katoch, S. S. Chauhan, and V. Kumar, “A review on genetic algorithm: past, present, and future,” *Multimedia Tools and Applications*, vol. 80, pp. 8091–8126, 2021.
- [12] S. Gillies, C. van der Wel, J. V. den Bossche, M. W. Taves, J. Arnott, B. C. Ward *et al.*, “Shapely,” 2024. [Online]. Available: <https://github.com/shapely/shapely>
- [13] A. F. Gad, “Pygad: An intuitive genetic algorithm python library,” *Multimedia Tools and Applications*, pp. 1–14, 2023.
- [14] S. B. Remman, “Realistic LiDAR Counterfactuals,” 2024. [Online]. Available: https://github.com/sbremman/realistic_lidar_counterfactuals
- [15] A. Raffin, A. Hill, A. Gleave, A. Kanervisto, M. Ernestus, and N. Dormann, “Stable-baselines3: Reliable reinforcement learning implementations,” *J. Mach. Learn. Res.*, vol. 22, no. 268, pp. 1–8, 2021.
- [16] T. Haarnoja, A. Zhou, K. Hartikainen, G. Tucker, S. Ha, J. Tan, V. Kumar, H. Zhu, A. Gupta, P. Abbeel *et al.*, “Soft actor-critic algorithms and applications,” *arXiv preprint arXiv:1812.05905*, 2018.
- [17] J. Tobin, R. Fong, A. Ray, J. Schneider, W. Zaremba, and P. Abbeel, “Domain randomization for transferring deep neural networks from simulation to the real world,” in *2017 IEEE/RSJ International Conference on Intelligent Robots and Systems (IROS)*. IEEE, 2017, pp. 23–30.
- [18] N. Koenig and A. Howard, “Design and use paradigms for Gazebo, an open-source multi-robot simulator,” in *Proceedings of the IEEE/RSJ International Conference on Intelligent Robots and Systems (IROS)*, vol. 3. IEEE, 2004, pp. 2149–2154.
- [19] S. B. Remman, “Turtlebot3 random navigation environments,” 2024. [Online]. Available: https://github.com/sbremman/turtlebot3_random_navigation_environments
- [20] S. Remman and A. Lekkas, “Using Shapley additive explanations to explain a deep reinforcement learning agent controlling a TurtleBot3 for autonomous navigation,” in *Proceedings of the 21st International Conference on Informatics in Control, Automation and Robotics - Volume 1*, 2024, pp. 334–340.
- [21] T. Akiba, S. Sano, T. Yanase, T. Ohta, and M. Koyama, “Optuna: A next-generation hyperparameter optimization framework,” in *Proceedings of the 25th ACM SIGKDD International Conference on Knowledge Discovery & Data Mining*, 2019, pp. 2623–2631.
- [22] R. K. Mothilal, A. Sharma, and C. Tan, “Explaining machine learning classifiers through diverse counterfactual explanations,” in *Proceedings of the 2020 Conference on Fairness, Accountability, and Transparency*, 2020, pp. 607–617.